

## Peer review status:

This manuscript is a non-peer reviewed preprint submitted to EarthArXiv.

#### Title

Eocene lacustrine-volcaniclastic deposits at Aliabad (Central Iran): A possible Protobasin of the Oligo-Miocene Qom Formation

## **Authors & Affiliations**

Mahdokht Karimi¹ (<u>m19 karimi@ut.ac.ir</u>, <u>mahdokhtkarimi19@gmail.com</u>)
Abdolhossein Amini¹ (<u>ahamini@ut.ac.ir</u>, <u>ahamini@gmail.com</u>)
Nasrollah Abbassi² (<u>abbasi@znu.ac.ir</u>, <u>nasrabbassi@gmail.com</u>)
Mohsen Ranjbaran¹ (<u>m.ranjbaran@ut.ac.ir</u>)

- 1. School of Geology, College of Science, University of Tehran, Tehran, Iran
- 2. Department of Geology, Faculty of Science, University of Zanjan, Zanjan, Iran

# **Corresponding Author**

Mahdokht Karimi, m19 karimi@ut.ac.ir

# **Journal Submission Status**

This manuscript is intended to be submitted to *Episodes, Journal of international Geoscience* 

# Mastodon Handle

@mah\_karimi

# Eocene lacustrine-volcaniclastic deposits at Aliabad (Central Iran): A possible Proto-basin of the Oligo-Miocene Qom Formation

#### Authors:

Mahdokht Karimi<sup>1\*</sup>, Abdolhossein Amini<sup>1</sup>, Nasrollah Abbassi<sup>2</sup>, Mohsen Ranjbaran<sup>1</sup>

#### Affiliations:

- 1. School of Geology, College of Science, University of Tehran, Tehran, Iran
- 2. Department of Geology, Faculty of Science, University of Zanjan, Zanjan, Iran

#### 1. Abstract

Central Iran hosts intricate Cenozoic successions where the Oligo-Miocene Qom Formation forms major hydrocarbon reservoir. The stratigraphic and paleoenvironmental relationship of the Eocene Aliabad deposits to this formation has been controversial. This study integrates stratigraphic logging, petrography, geochemistry (XRD/XRF), and ichnology on 46 thin sections from Aliabad and 157 comparative samples from the Qom Formation to determine age, composition, stratigraphic, petrographic, diagenetic, diagenesis and depositional environment. Results demonstrate that the Aliabad deposits are exclusively Eocene, dominated by hybrid volcaniclasticcarbonate facies (with a mean content of ~69 % volcaniclastic content), lacking Oligo-Miocene index fossils. Geochemical data reveal primary volcanic minerals (albite, microcline) and abundant secondary alteration and evaporite phases (analcime, clinoptilolite, halite, carnallite, hematite). Diagenesis involves volcanic glass alteration to clays and zeolites, diverse cements, dissolution, neomorphism, compaction, pyritization and limited dolomitization. Sedimentological and ichnological evidence of *Thalassinoides* indicate a predominantly lacustrine environment with episodic marine incursions and pyroclastic events. Together, these results confirm that Aliabad is a distinct Eocene lacustrine-volcaniclastic basin unrelated to the Oligo-Miocene marine carbonate ramp of the Qom Formation and highlight potential evaporite and iron-oxide mineralization.

Keywords: Central Iran, Aliabad sediments, Qom Formation, Volcaniclastic-carbonate, Lacustrine paleoenvironment

<sup>\*</sup>Corresponding author: Mahdokht Karimi, Department of Geology, School of Science, University of Tehran, Iran. E-mail: m19\_karimi@ut.ac.ir

#### 2. Introduction

Central Iran's Cenozoic stratigraphy is complex, featuring multiple unconformities and varied depositional environments [29, 38]. In particular, the Aliabad locality, situated roughly 35 km north of Qom, exposes a tectonically uplifted sequence of carbonate, mixed volcaniclastic—carbonate and pyroclastic rocks that record both marine and lacustrine facies [46]. The Eocene succession at Aliabad includes thick volcanic and tuff units (>3 km) [20, 21] interrupted by limestone and marl horizons, reflecting episodes of intense volcanism and tectonism during the Middle Alpine orogeny [20, 21]. This lithological and palaeontological heterogeneity, along with distinctive trace-fossil assemblages, contrasts sharply with the contemporaneous Qom Basin [41].

The Oligo-Miocene Qom Formation a late Oligocene to early Miocene shelfal—upper slope marine carbonate—dominated unit [24, 25, 52], broadly equivalent to the Asmari Formation of the Zagros fold belt [13, 43, 44], represents a transgressive shallow-marine carbonate ramp that overlies either the Lower Red Formation or Eocene volcanics [5]. It contains fore-reef, reef, lagoonal and basin-margin facies [31, 51] and reaches thicknesses up to 2.3 km [19], making it a major hydrocarbon reservoir and source rock [32]. Although the Qom Formation and Aliabad locality are geographically close, their depositional, tectonic and diagenetic histories differ markedly; the nature and stratigraphic position of the Aliabad sediments relative to the Qom Formation remain unclear. Resolving whether Aliabad represents a separate Eocene lacustrine—volcaniclastic basin or a proto-Qom basin is critical for reconstructing Central Iran's Cenozoic palaeogeography and for assessing the region's resource potential.

This study therefore adopts an integrated field and laboratory approach to explore the Aliabad–Qom connection. Stratigraphic sections were measured across five Aliabad outcrops; petrographic, geochemical (XRD/XRF) and paleontological samples were collected; and ichnological observations were made. These data are combined to characterise the lithology, diagenesis and depositional setting of the Aliabad deposits and to compare them systematically with adjacent Qom Formation facies. Although limited field access and the fine-grained nature of some facies constrained sampling and isotopic analyses, the integrated dataset provides a robust basis for interpreting basin evolution. By clarifying the relationship between Aliabad and the Qom Formation, the work aims to refine models of Central Iran's tectono-stratigraphic development and to guide future exploration of evaporite, iron-oxide and hydrocarbon resources.

# 3. Geological Setting

## **Aliabad Region**

The Aliabad study area consists of five relatively continuous successions with little deformation and limited exposure in five stratigraphic sections (Fig. 1).

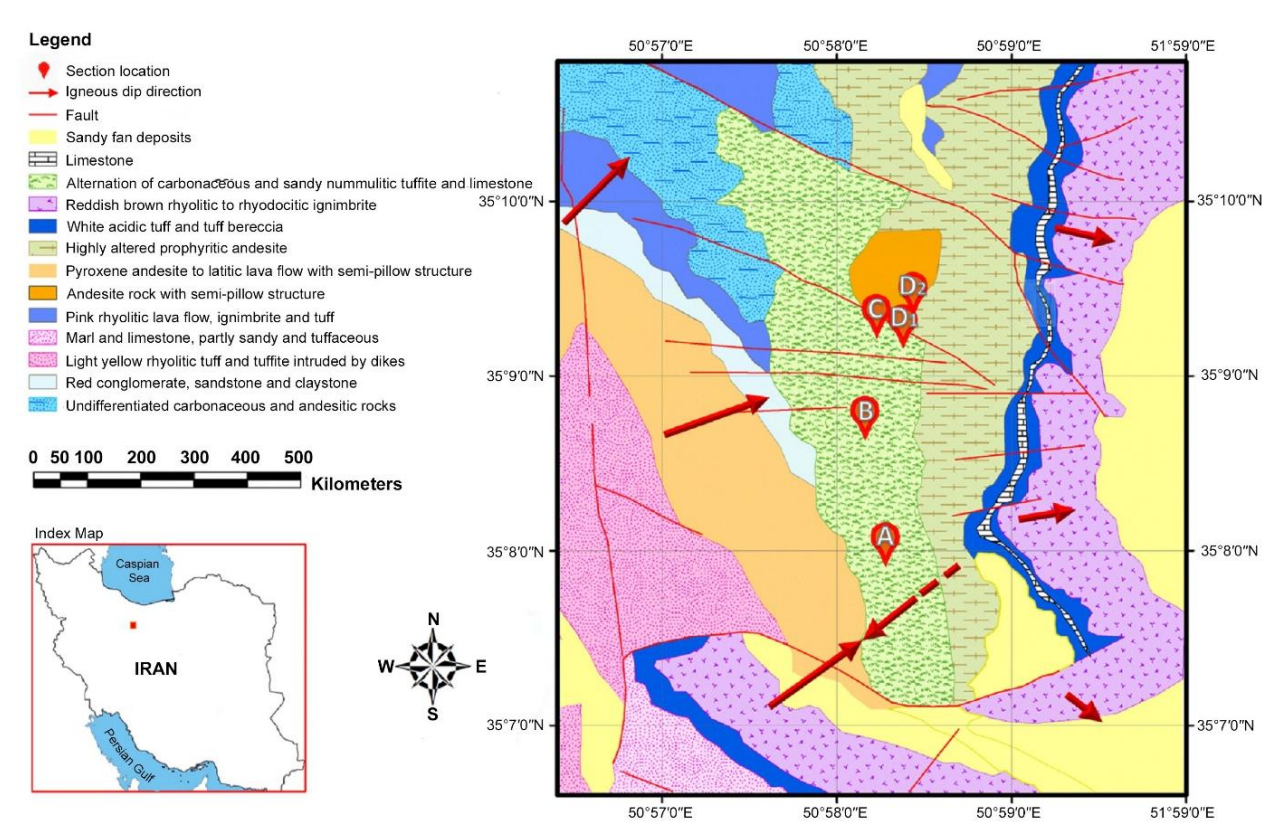


**Fig 1. Lithological distribution map of the Aliabad–Qom region.** The map shows the main lithological units, faults, and igneous dip directions, together with measured section locations (A–D). Units include sandy fan deposits, limestone, alternations of carbonaceous and sandy nummulitic tuffite and limestone, rhyolitic to rhyodacitic ignimbrites, acidic tuffs and tuff breccias, porphyritic andesites, pillow-like andesitic lavas, rhyolitic lava flows and ignimbrites, marl and tuffaceous limestone, rhyolitic tuffs intruded by dikes, red conglomerates, sandstones and claystones, and undifferentiated carbonaceous—andesitic rocks. These lithologies illustrate the complex interplay of volcanism, sedimentation, and tectonics in the Aliabad–Qom basin. The inset map shows the regional location of the study area within Iran [27].

The Cenozoic stratigraphy of Central Iran reveals extensive unconformities during the transitional interval from the end of the Cretaceous to the beginning of the Paleocene [29]. Eocene sequences are volcanically disturbed and discontinuous, with the earliest Lutetian fossil-bearing horizons [25]. Heterogeneity of lithology and fossils characterize varied paleogeographic conditions [5]. Volcanism and tectonism of Middle Alpine orogeny generated extensive instability [15].

Lower Eocene volcanic rocks and tuffs (>3000 m) [20, 21] comprise the thickest successions at Aliabad, for instance, eight nummulitic horizons [29]. Regionally, there is lateral passage from Eocene Lutetian limestone—marl successions [25, 59] to gypsiferous and volcanic facies in Semnan and south of Qom. Hajian [29] divided Tafresh Eocene

deposits into six lithozones (E1–E6), varying from red clastics with basal nummulites to thick Upper Eocene units of volcanic [14], tuffitic, and limestone-bearing composition.

Pyrenean tectonics started transgression of the sea over the western Central Iran zone in the Oligocene–Miocene, resulting in evaporitic Lower Red Formation deposits and transgressive Oligo-Miocene carbonates [20, 21]. These limestones, Asmari Formation facies-equivalent, are significant hydrocarbon reservoirs [5].

In terms of structural setting Iran is situated at a crucial segment of the Alpine–Himalayan orogenic belt, and Central Iran is a long-term, structurally complex tectono-sedimentary region [6, 11, 12, 47, 53]. Regional structural trends are NW–SE-oriented with the Urumieh–Dokhtar zone, where folding and strike-slip faulting prevail [6, 7, 44]. Progressive orogenies—Laramide, Pyrenean, and Pasadenian—governed subsidence, volcanism, and basin evolution [45, 47].

A sequence of major active and ancient faults surrounds the Aliabad–Qom area [58], some of which are shown in Figure 1. The Bid-e-Hend, Ravand, Alborz, Qom, Davazdah Emam, Siah Kooh, and Koushk-e-Nosrat faults are all NW–SE trending strike-slip faults having a vast majority showing transtensional pull-apart basins or thrusting [15, 20, 28]. These faults control sedimentation, volcanism, and reservoir architecture [26].

#### **Qom Formation**

The Qom Formation, which was deposited following Pyrenean orogeny (Middle Oligocene–Early Miocene), occurs on the Lower Red Formation or Eocene volcanics and attains thicknesses of up to 2300 m [17, 19, 36, 37]. It is a transgressive shallow-marine to marine carbonate ramp with fore-reef, reef, lagoonal, and basin-margin facies [18, 48]. Stratigraphic cycles (I–III) have been identified [5, 43, 49].

Variability of facies indicates local tectonic and volcanic contribution, hypersaline lagoonal to shallow-marine conditions prevailing in Eyvanki, Kashan, and Navab anticline sections [4, 10]. Regional change in facies is an indicator of basin depositional initiation and connectivity variability [48].

Economically, the Qom Formation is an exceptionally prolific hydrocarbon reservoir, as is seen in the Alborz oil field [5] and Sarajeh gas field [3]. Its co-occurring celestite and gypsum deposits reflect its evaporitic facies potential [33].

## 4. Methods and Materials

This study was carried out over a period of ~2 years, incorporating 10 separate field campaigns conducted in the Qom Basin and surrounding areas. Each campaign combined detailed fieldwork with targeted laboratory analyses, and subsequent campaigns built on earlier results through iterative sampling, petrographic examination,

and geochemical testing. In total, more than 200 thin sections and multiple geochemical datasets were generated and integrated with structural and stratigraphic observations to reconstruct the depositional and diagenetic history of the Aliabad and Qom formations.

#### Field investigations

During each field season, stratigraphic sections were measured and described in detail from well-exposed outcrops. Observations included lithological variability, bed thickness, lateral continuity, dip, sedimentary structures, and fossil content. These data were used to construct measured stratigraphic columns, which provided the framework for sampling. Field campaigns were iterative, with later surveys refining previous measurements and targeting specific lithologies for additional collection.

## Sampling strategy

Samples collected during the field campaigns were supplemented by exploration-company archives and university collections, ensuring that the dataset covered a wide range of lithologies and stratigraphic levels. This approach yielded 203 thin sections:

- Aliabad exposures (approximately 35 km north of Qom): 46 thin sections from five stratigraphic sections (red symbols, in Figure 2).
- Qom Formation outcrops (Tehran–Qom highway corridor): 29 thin sections from two limestone localities, including Aliabad Caravanserai (green symbols, in Figure 2).
- Exploration-company collections: 49 thin sections from Davazdah-Emam, 48 from Separ-Rostam, and 19 from Kaj (yellow symbols, in Figure 2).
- University of Tehran archives: 12 thin sections of the region from departmental collections (blue symbols, in Figure 2).



**Fig 2. Study Area Outcrop and Sampling Location Map.** Satellite image map illustrating the geographical location of the studied outcrops and various sampling points within the research area. The locations of the various sample collections are distinguished by the following color-coded triangular symbols: Red symbols denote the locations of the Aliabad deposits outcrops. Green symbols mark the locations of the Qom Formation outcrops that were examined and measured in the field. Blue symbols indicate the locations from which university thin section samples were collected for laboratory analysis. Yellow symbols represent the sites of exploration-company collections from the nearest exposures of the Qom Formation. Scale bar (bottom left, 22.788 km) North arrow (top right). (Note: This map highlights both field-measured outcrops and specific sample collection points for detailed study and is modified from the original source [54].)

## Petrographic analysis

Thin-section petrography was the most time-intensive component of this study and. A total of 203 thin sections were prepared and systematically examined under transmitted-light microscopy at magnifications ranging from 25× to 400×. Petrographic analysis followed the facies terminology of Flügel [23], which provided a consistent framework for documenting textures, fossil content, and diagenetic features.

The work was iterative: initial batches of thin sections were described during the first phase of the project, with subsequent field seasons adding new material that required cross-comparison with earlier descriptions. Each thin section was logged in detail, noting fabric, grain types, fossil associations, cement phases, and alteration. Quantitative point-counting was applied to a large subset of sections, typically 250–400 counts per slide, to establish statistically reliable proportions of carbonate vs. volcaniclastic material [55]. This alone represented months of microscope work spread across multiple phases of the project. Alizarin Red S staining was used selectively but strategically to highlight calcite,

dolomite, and diagenetic cement phases, especially where optical identification was ambiguous [16].

### Geochemical and mineralogical analysis

Geochemical and mineralogical analyses complemented petrography by constraining mineral assemblages and chemical composition, particularly in fine-grained lithologies and volcaniclastic intervals [30, 39, 42]. Powdered samples were prepared from hand specimens and thin-section offcuts, with care taken to avoid contamination from surface weathering [1]. X-ray diffraction (XRD) analysis was conducted on selected samples to determine bulk mineralogy, focusing on clay-rich facies and tuffaceous horizons [30, 35]. The XRD results were used to identify crystalline phases, discriminate between carbonate polymorphs, and detect secondary minerals related to alteration [56].

X-ray fluorescence (XRF) spectroscopy was applied to the same set of samples to obtain major- and trace-element concentrations [50, 57]. These data provided insights into provenance and depositional setting, as well as into the degree of volcanogenic input, particularly in the distinctive green tuff horizons [8]. The tuffaceous layers were analyzed in detail because they represent key time-stratigraphic surfaces within the succession and provide evidence for syn-depositional volcanic activity [42]. Geochemical fingerprints from these horizons were used both for stratigraphic correlation and for interpreting volcanic influence on sedimentation [9, 30].

# **Data integration**

The final stage of analysis involved integrating the field, petrographic, and geochemical datasets with structural context to develop a coherent reconstruction of basin evolution. Lithological descriptions from the field provided the framework into which petrographic and geochemical observations were incorporated. Facies distributions were compared across sections to identify lateral and vertical trends in depositional environments.

Diagenetic features documented in thin section were considered in relation to structural measurements from the field, allowing assessment of the timing of dolomitization, cementation, and recrystallization relative to tectonic deformation. Geochemical results, particularly from the tuffaceous horizons, were cross-referenced with petrographic data to validate the interpretation of depositional settings and volcanic influence.

This integrative approach made it possible to compare the Aliabad and Qom Formation successions on a common basis. Key differences in facies architecture, lithological composition, and diagenetic imprint were highlighted, while similarities provided evidence for basin-wide controls. The combined dataset thus supported the reconstruction of depositional systems, diagenetic pathways, and broader paleoenvironmental evolution in the Qom Basin

#### 5. Results

#### 5.1 Aliabad Region

#### Fine-grained analysis

Stratigraphic columns from Aliabad (Fig. 3) and the adjacent Qom Formation (Fig. 8) outcrop (Section Q) together with field measurements provided the framework for petrographic and geochemical studies. Fine-grained samples from Section D were stained with Alizarin Red S and analyzed using XRD and XRF (Fig S1, Tables S1 and S3-S4, and Fig. 4A). These analyses confirmed the dominance of carbonate mineral phases and revealed the presence of K-feldspar, consistent with earlier reports of volcanogenic input into the basin [60].

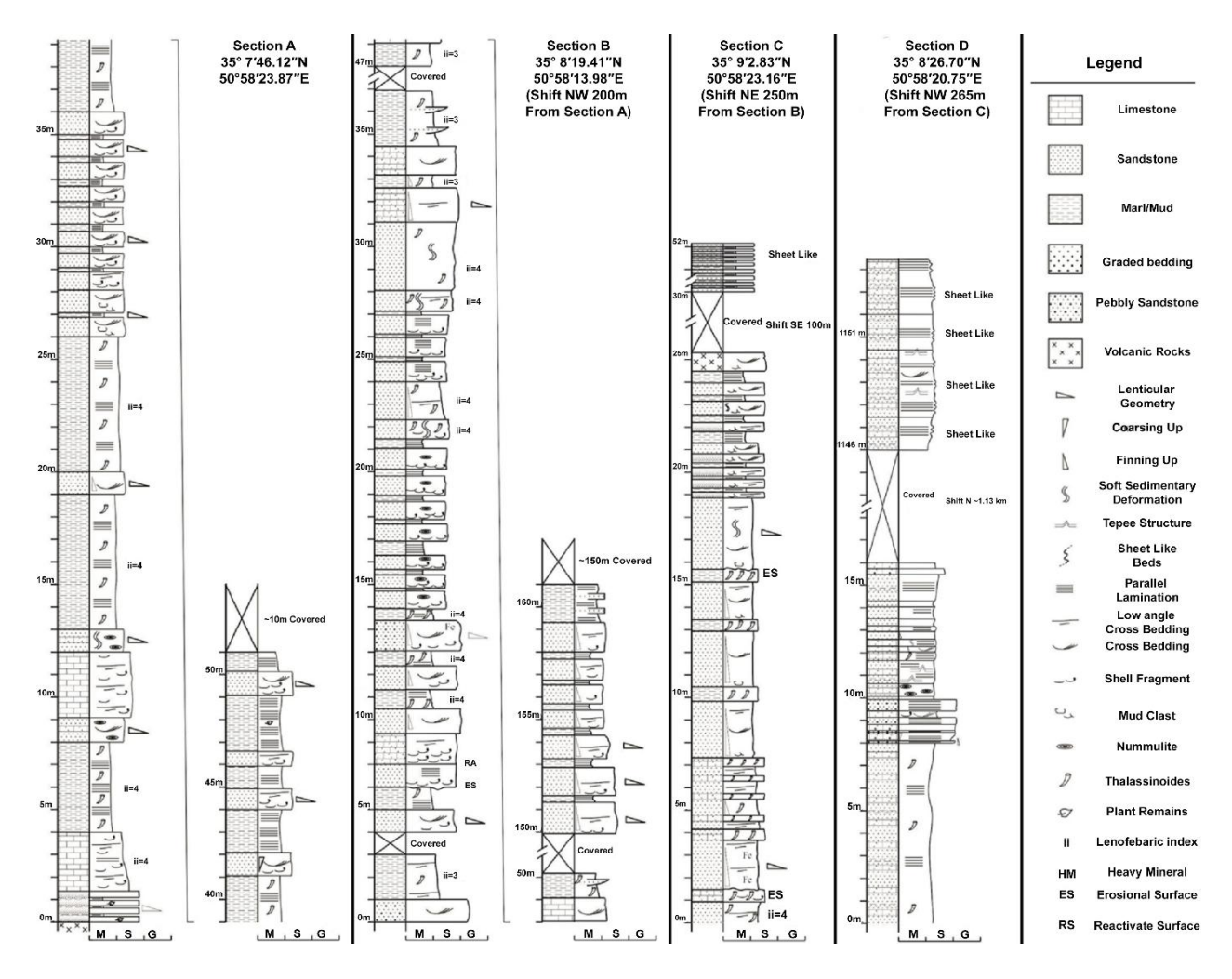


Fig 3: Stratigraphic Columns and Detailed Lithological Successions of Sections A, B, C, and D of the Aliabad. The columns are constructed from detailed field measurements and are modified after Abbassi and Amini [2]. These sections document the vertical architecture of the formation, highlighting changes in lithology, sedimentary structures, and biotic components. The vertical scale is in meters (m), and the basal

horizontal axis indicates the general grain size distribution for the bottom of the columns: Mud, Sand, and Gravel.

### **Volcaniclastic components**

Tuffaceous rocks are a major constituent of the succession. Among the total 46 samples examined, lithic and crystal tuffs are most frequent, whereas vitric-crystal tuffs are least abundant. Across all sections, volcaniclastic components average 69.02% of the total rock volume (Table S2, Fig. 4B and 4C). Bulk-oxide and trace-element compositions determined by XRF (Table S3-S4, Fig. 4D and 4E) further highlight the substantial volcanic contribution to the Aliabad succession.

#### **Hybrid arenites**

The mixed character of the deposits is reflected in their classification as Hybrid Arenites [61, 62]. Petrographic examination identified both intrabasinal carbonate components (ooids, peloids, micritic intraclasts, and fossils) and extrabasinal non-carbonate fragments, particularly volcanic grains (quartz, K-feldspar, plagioclase, and pyroclastic lithics). Interstitial material includes both carbonate (calcite, dolomite) and non-carbonate (quartz, phyllosilicate, iron oxide) cements, as well as carbonate micritic matrix. The distribution of these components (Table 1) indicates that the Aliabad deposits plot between the CI (Intrabasinal Carbonate) and NCE (Extrabasinal Non-Carbonate) poles of Zuffa's Scheme [62].

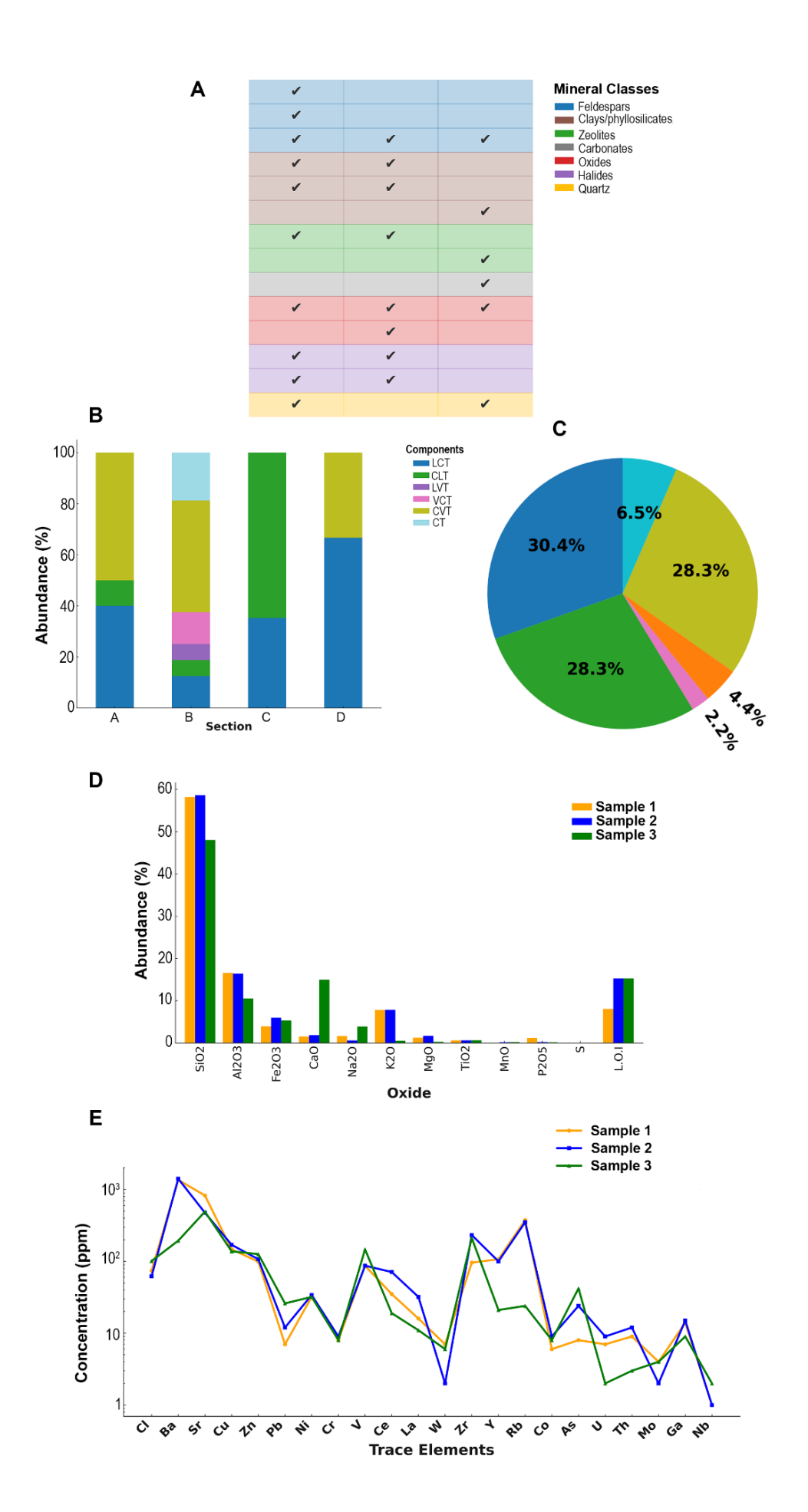


**Fig 4.** Geochemical and mineralogical characteristics of the Aliabad succession. **A)** Mineralogical presence/absence chart based on XRD analysis, grouped and color-coded by mineral class (feldspars, clays, zeolites, carbonates, oxides, halides, and others).  $\checkmark$  indicates presence of a given phase in each sample. **B)** Stacked bar diagram showing the distribution of volcaniclastic component types (LCT, CLT, LVT, VCT, CVT, CT) across measured sections (A–D). **C)** Pie chart illustrating the overall proportion of volcaniclastic component types in all sections combined. **D)** Major oxide composition (wt.%) of representative samples from bulk geochemical analyses, highlighting dominant SiO<sub>2</sub> and Al<sub>2</sub>O<sub>3</sub> contents with variable CaO, K<sub>2</sub>O, and LOI. **E)** Multi-element spider plot of trace element concentrations (ppm) plotted on a logarithmic scale, showing comparable enrichment–depletion patterns among the three samples.

**Table 1.** Petrographic identification and classification of constituent components in regional deposits rocks according to zuffa's [62] hybrid arenite framework

From Zuffa's Scheme		Enomo o vica els	Extrabasinal	NCE (Non- carbonate)
NCE	ဟ	Framework Component	Intrabasinal	CI (Carbonate)
			Extrabasinal and	V (Volcanic
itine			or Intrabasinal	Grains)
	Main Constituents	Interstitial Component		CCm (Carnonate
			Cement	Cement)
HA HA				NCCm (Non-
				carbonate
CI NCI				Cement)
			Matrix	CMt (Carbonate
			IVIALIIX	Matrix)

## Diagenetic features

Thin-section analysis documents a wide range of diagenetic processes affecting both carbonate and volcaniclastic fractions. Micritization, cementation, neomorphism, dissolution, compaction, fracturing, pyritization, and limited dolomitization are all observed. Bioturbation structures, including *Thalassinoides* burrows, occur at multiple scales (Figures 5, 6A–B).

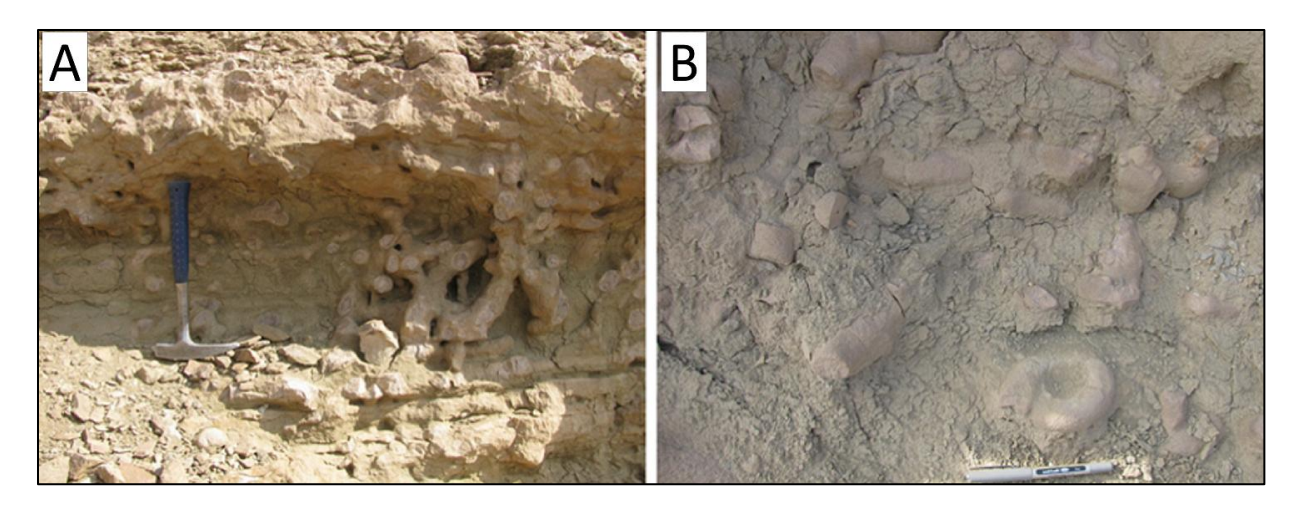


**Fig 5. A)** Scaffolded *Thalassinoides* trace fossil from Section C, showing complex burrow structures indicative of intense bioturbation. **B)** Another occurrence of *Thalassinoides* trace fossil identified in Section A.

Cements include blocky, drusy, syntaxial overgrowths, and dogtooth calcite, as well as silica, chalcedony, and iron oxides (Figures 6C–L). Neomorphic microsparite and pseudosparite are common (Figure 6M). Dissolution features and meteoric cement fills are widespread (Figures 6O–P). Compaction ranges from mechanical breakage of grains to stylolitization (Figures 6Q–R), while fractures are variably filled with calcite or chalcedony (Figures 6N, 6H). Early framboidal pyrite and vein-filling pyritization are present (Figures 6S–T). Dolomitization is rare, limited to fracture-filling replacement (Figure 6W). Volcaniclastic diagenesis is marked by alteration of volcanic glass to clays, zeolites, and palagonite, feldspar turbidization, and secondary silica/zeolite cementation (Figures 6U–V). These processes correspond to sequential marine, meteoric, and burial diagenetic settings (Table 2).

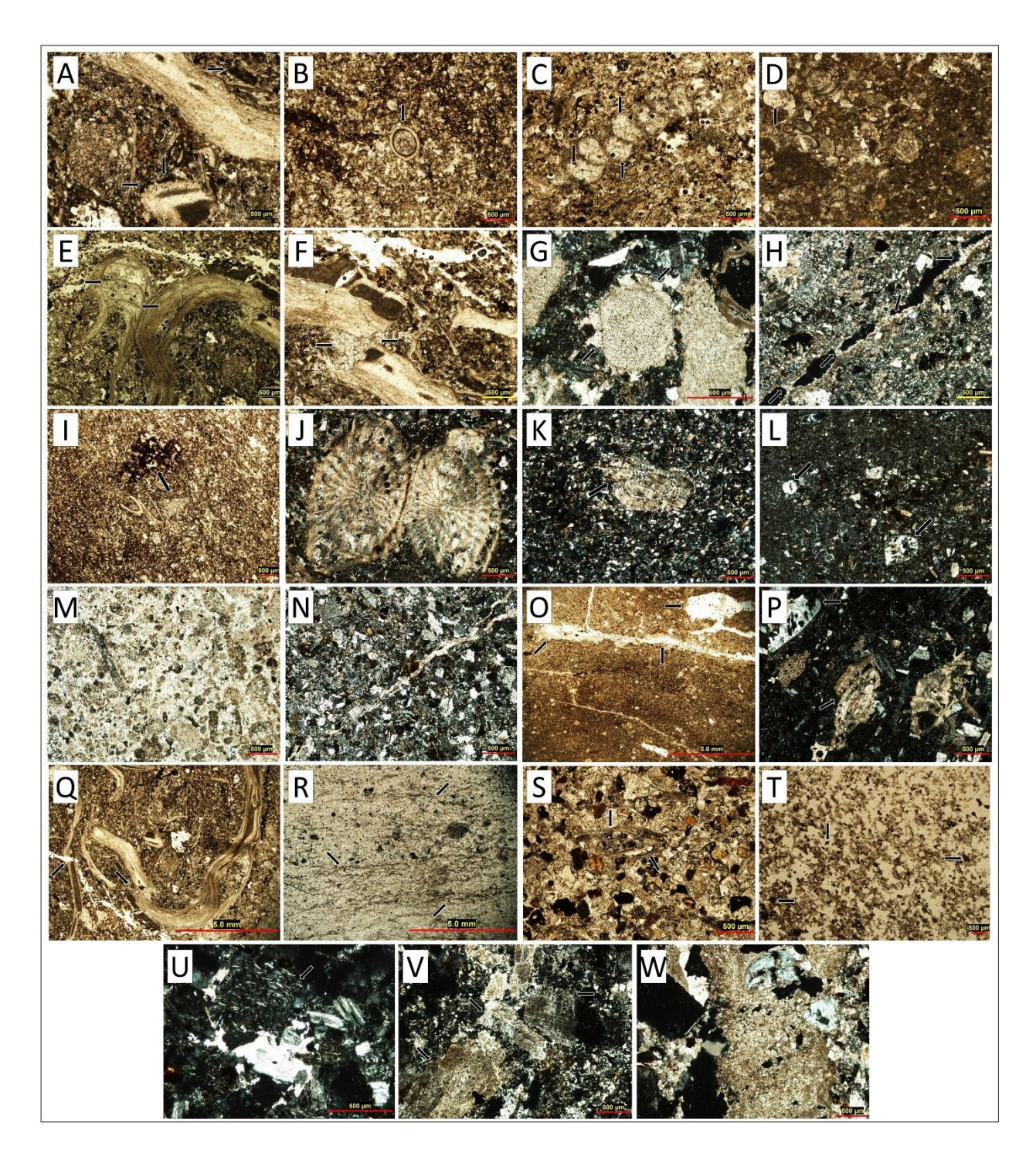


Fig 6. A) A fully micritized fragment (top) and micritization along the margin of a skeletal fragment (bottom) (RMF28). B) Cross-section of a worm tube (a type of bioturbation at the microscopic scale) (RMF5). C) Blocky cement filling the pores of skeletal components (RMF13). D) Blocky cement filling the pores of skeletal components (RMF30). E) Drusy cement filling the pores of a mollusk skeletal fragment (RMF28). F) Drusy cement filling a void created by fracturing (RMF28). G) Syntaxial Calcite Overgrowth Cement surrounding an echinoderm fragment (RMF13). H) Cement precipitated along a fracture ridge in a volcaniclastic rock containing approximately 40% carbonate components (RMF13), which appears to have

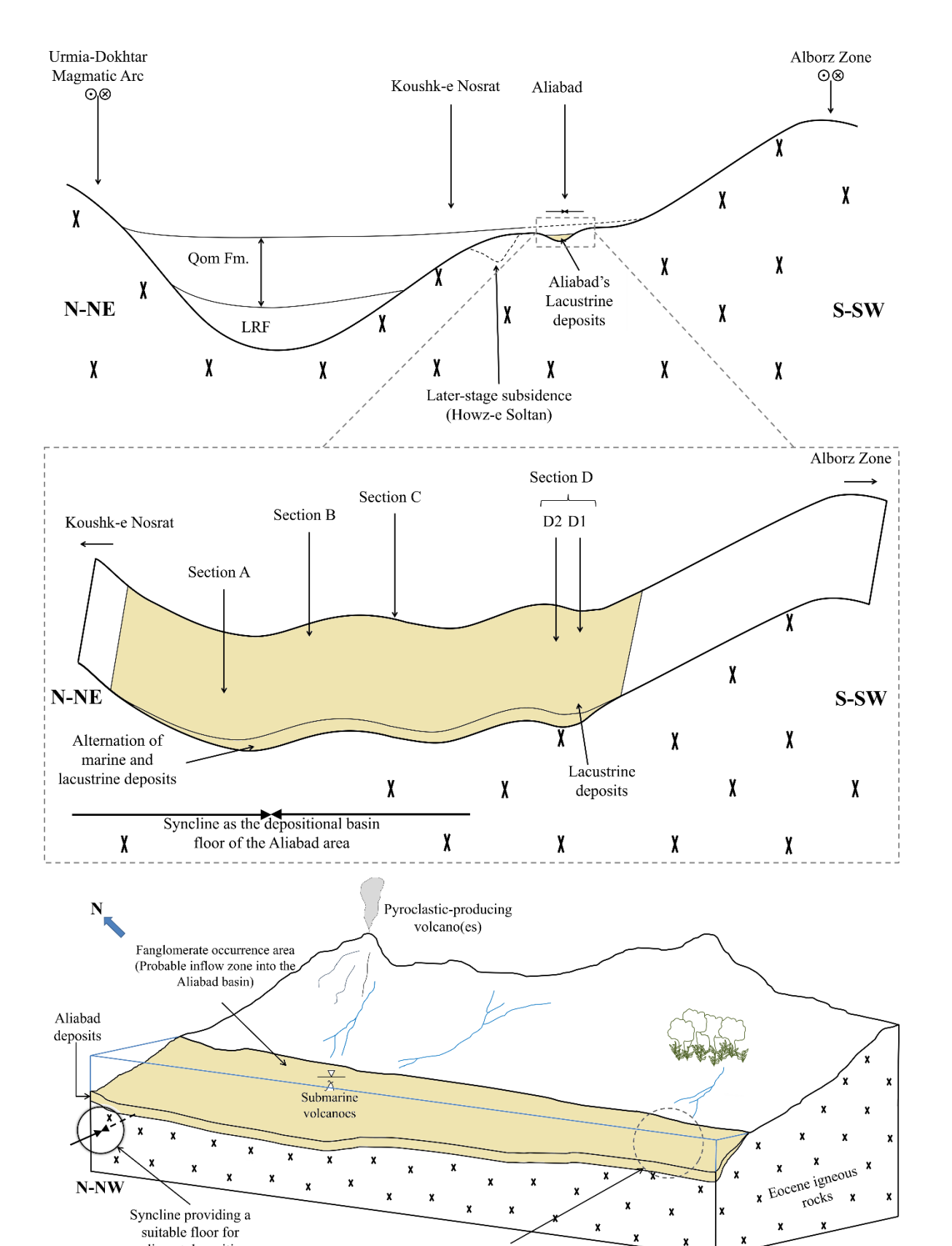
formed following a phase of dissolution. I) Iron oxide cement (RMF2). J) Siliceous cement filling the pores of foraminifera (RMF13). K) Chalcedony cement replacing the walls of a foraminifer within a volcaniclastic rock containing only about 10% carbonate components. L) Chalcedony cement filling voids in a volcaniclastic rock. M) Occurrence of neomorphism and transformation of fine-grained particles into pseudosparite calcite cement (RMF29). N) Calcite-filled fracture in a volcaniclastic rock. O) Dissolution along fractures (RMF13). P) Skeletal fragments (Nummulites) undergoing dissolution and degradation within a volcaniclastic rock. Q) Fragmented skeletal components resulting from mechanical compaction (RMF28). R) Dissolution seams formed by chemical compaction in a recrystallized limestone. S) Framboidal pyrite precipitated within the pores of a foraminifer in a volcaniclastic rock containing 30% carbonate particles. T) Framboidal pyrite in a volcaniclastic rock with approximately 25% recrystallized carbonate. U) Palagonite formed by the alteration of volcanic glass. V) Decomposing feldspars exhibiting a sieve-textured and dusty appearance. W) Dolomite filling a fracture in a crystal-vitric tuff (volcaniclastic rock).

**Table 2.** Probability of diagenetic stages in different diagenetic environments in Aliabad region (adapted from Flügel [23]) Legend: ■: Presence in environment, ■: Presence in shallow environment, □: Rare presence in environment.

		Eodiagenesis				Meso- diagene sis	ene Telodiagenesis		
			Marine		Bui	rial	Mete	eoric	
		Ph	reatic						
Diagenetic Processes				Vadose	Shallow	Deep	Phreatic	Vadose	
Micritiz	zation			-	-	-	-	-	
Blocky (					ı				
Overgrowt		-			-	-	-		
Drusy C		-	-	-		-		-	
Dogtooth		-	-	-		-		-	
Pseudo (Neomo		-	•	-	-	ı	-	-	
Disso	lution		-	-	-		O		
Compostion	Grain Fracturing	-	-	-		ı	-	-	
Compaction	Dissolution Vein	-	-	-	•	ı	-	-	
Fracturing of	Fracturing of Rock Mass		-	-		1	-	-	
Pyritiz	Pyritization		-	-	-	-	-	-	
Dolomit						1			
Bioturl ( <i>Thalass</i>	bation sinoides)	-		-	-	-	-	-	
Alteration of v	olcanic glass			·		0		•	

#### **Depositional environment**

Field relationships, fossil content, and petrographic data indicate that the Aliabad basin was a lacustrine system subject to synclinal subsidence and high volcaniclastic influx. Plant macrofossils and crab traces point to shallow-lake conditions with intermittent marine connections. Local variations include turbiditic beds in Section A (deepening events), hydroclastic deposits in Section C (submarine vents), and fanglomerates (fluvial input). Rounded pyroclastic grains and epiclastic textures reflect littoral eruptions, while poorly sorted volcaniclastics interbedded with pelagic sediments indicate aqueous transport and deposition [20, 22]. Collectively, these features suggest a dynamic pyroclastic—carbonate mixed lake system episodically linked to marine incursions and contemporaneous volcanism (Fig. 7, Table 3).



Probable entry zone of plant

material into the basin

(southeastern margin of the basin)

S-SE

sediment deposition

**Fig 7. Top.** A schematic regional cross-section from north–northeast to south–southwest, extending from the Urumieh–Dokhtar Magmatic Arc to the Alborz Zone, showing the structural position of the Aliabad succession relative to the Qom Formation and associated later-stage subsidence. **Middle.** Enlarged view of the Aliabad area illustrating the internal architecture of the basin, including measured sections (A–D) and the alternation of lacustrine and marine deposits accumulated within a synclinal depression that acted as the depositional floor. **Bottom.** Conceptual sedimentary model of the Aliabad lacustrine basin, depicting volcaniclastic input from pyroclastic-producing volcanoes, the development of submarine volcanic centers, probable fan–delta and conglomerate feeder systems, and localized input of plant material along the southeastern margin of the basin.

 Table 3: Investigation of the Characteristics of Volcano Types and Water-Related Explosive Events, and

Their Correlation with the Deposits of the Aliabad Region.

Magmatic Eruption  Type Properties	Submarine Eruptions	Nearshore or Littoral Eruptions	Correlation with the Geological Setting and Rock Types of the Aliabad Region
Glass Abundance	✓	×	<ul> <li>(Not in abundant or sufficient quantity)</li> </ul>
Fine-Grained Texture	✓	✓	✓
Abundant Vesicles	<b>√</b>	×	× (Only in Section C and Locally)
Formation Environment and Explosive Events	The aforementioned locations above	In various locations	Back-Arc Basin = Compatible with Both
Grain Roundness Based on Composition	×	✓	✓

#### 5.2 Qom Formation

Stratigraphic sections south of Koushk-e Nosrat (Fig. 8) shows a transitional contact from Eocene volcanics to basal Qom limestones (member "a"), with local absence of the Lower Red Formation due to topographic control. Thickness variations are pronounced (Table S5) and partly fault-controlled along the Qom highway.

The basal **member a** consists of fossiliferous limestone with worm tubes, stylolites, and vertical fractures (~80 cm thick). Overlying this, **member b** comprises fine-grained limestones with sandy interlayers, bioturbation, cross-bedding, stylolites, and calcite-filled fractures, reaching thicknesses of more than 20 m. **Sub-member c1** is a sandy limestone containing volcanic clasts, abundant fossils, mud clasts, and stylolites (~7 m). Higher in the section, the **Upper Red Formation** appears abruptly and with substantial thickness. At the base, the contact with underlying **Eocene volcanics** is gradational, lacking Lower Red Formation deposits.

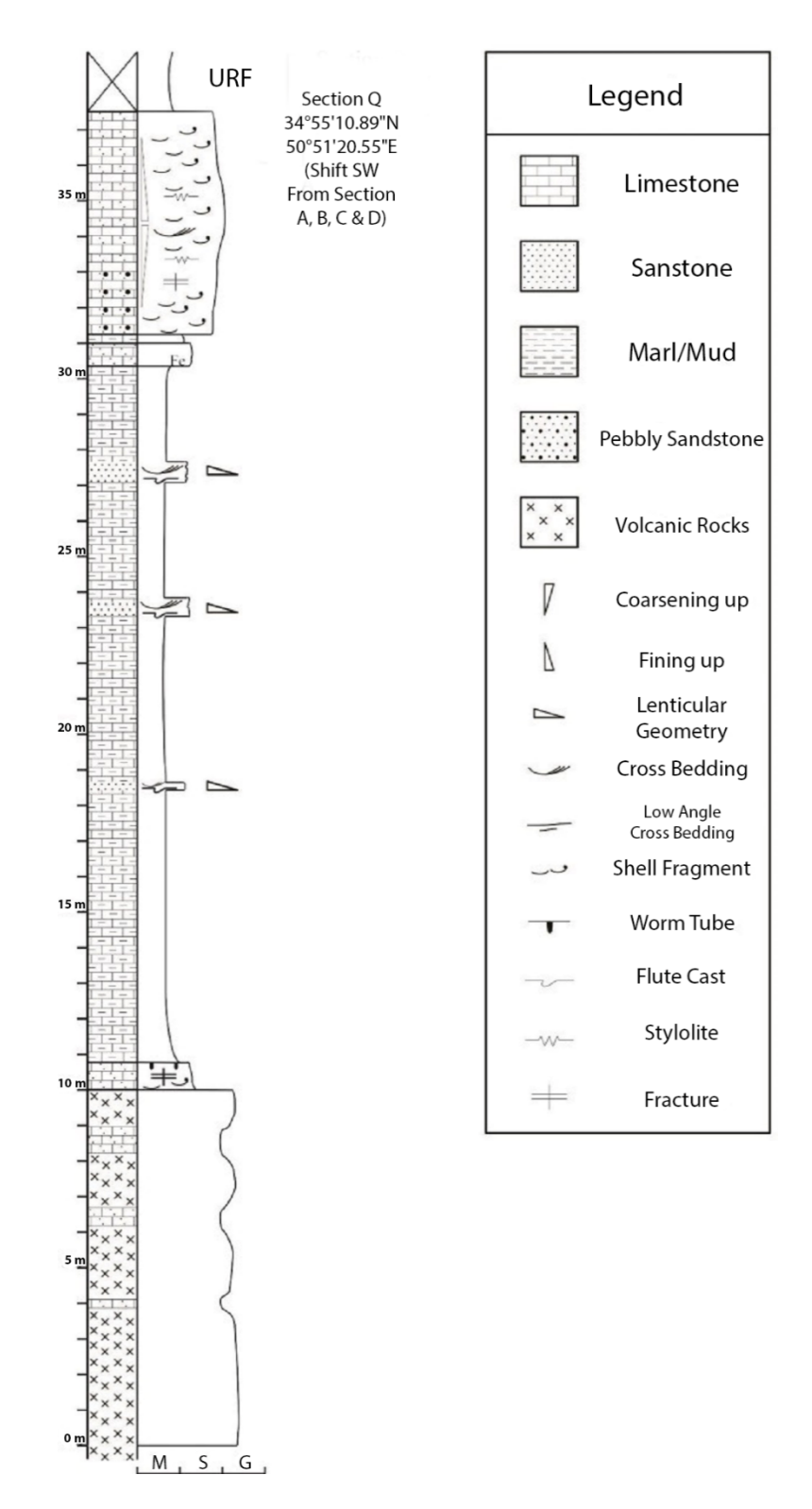


Fig 8: Stratigraphic Column of the Qom Formation (Section Q). Stratigraphic column measured from the Qom Formation outcrop, located south of Koshk-e Nosrat (Section Q). The coordinates for the measured section are  $34 \circ 55'10.89"N$  and  $50 \circ 51'20.55"E$ . The column illustrates the vertical succession of

lithologies and sedimentary features, extending from Volcanic Rocks at the base to the Unconformable Reference Formation (URF) at the top [34].

#### 6. Discussion

The primary aim of this study was to achieve a thorough characterization of the lithology, diagenesis, and depositional environment of the Eocene–Oligocene Aliabad sediments, and to unambiguously establish their distinction from the regionally significant Oligo-Miocene Qom Formation. Through extensive fieldwork supported by petrographic analysis, geochemical data (XRD, XRF), and paleoenvironmental interpretation, the study resolves long-standing ambiguities regarding the nature and stratigraphic position of the Aliabad succession.

## Hybrid volcaniclastic-carbonate system

Our findings categorically demonstrate that the Aliabad deposits represent a hybrid volcaniclastic—carbonate depositional regime. The high average volcaniclastic content (69.02%), dominated by lithic and crystal tuffs, reflects an active and dynamic volcanic source. The occurrence of hydroclastic deposits in Section C provides direct evidence for submarine eruptions within the basin. According to Zuffa's (32; 33) classification, these deposits are Hybrid Arenites, composed of both Intrabasinal Carbonate (CI: intraclasts, fossils, peloids) and Extrabasinal Non-Carbonate (NCE: volcanic clasts, quartz, feldspars) components, along with carbonate and non-carbonate cements and micritic matrix. The overall petrography, coupled with the presence of eodiagenetic phases such as pyrite, indicates that the dominant lithology is intrabasinal in origin but heavily modified by extrabasinal volcanic input.

#### Geochemical and diagenetic evolution

Geochemical analyses confirm a polymict mineral assemblage consisting of primary volcanic minerals (albite, microcline), alteration products (analcime, clinoptilolite, kaolinite, sericite), evaporites (halite, carnallite), and hematite and quartz. These assemblages record not only sustained volcanic influx but also restricted circulation and episodes of hypersalinity in the depositional system.

Diagenetic features reveal a complex post-depositional history influenced by alternating physicochemical regimes. Observed processes include micritization, diverse cement types (blocky, drusy, syntaxial, dogtooth, siliceous, chalcedony, iron oxide), neomorphism, dissolution, compaction, fracturing, pyritization, and limited dolomitization. Volcaniclastic diagenesis is marked by alteration of volcanic glass to clays, zeolites, and palagonite, producing secondary siliceous cements. These features collectively suggest sequential marine, meteoric, and burial diagenetic settings, with volcaniclastic alteration as the most distinctive diagenetic overprint.

#### Depositional setting and paleogeography

Sedimentological, ichnological, and paleontological evidence indicates that the Aliabad succession formed primarily in a lacustrine basin, influenced by synclinal subsidence and strong volcaniclastic supply. Vascular plant fossils and crab traces document shallow-lake conditions with periodic freshwater input, while fanglomerates mark fluvial influx during early basin development. Rounded pyroclastic grains and epiclastic textures indicate littoral-type eruptions, whereas turbiditic deposits in Section A point to rapid reworking of pyroclastic material, possibly near marine inlets.

Marine fossils and the dominance of *Thalassinoides* burrows—typical of shallow, highenergy marine-transitional environments—demonstrate episodic marine connections to the Eocene Sea. The Aliabad basin is therefore best interpreted as a multi-trophic lake system, ranging from shallow to deep facies, episodically invaded by marine waters and continuously affected by contemporaneous volcanism.

#### Distinction from the Qom Formation

The Aliabad succession differs fundamentally from the Oligo-Miocene Qom Formation, which represents an extensive marine carbonate ramp dominated by shallow-marine facies. In contrast, the Aliabad sequence records a lacustrine system with periodic marine intrusions and sustained volcanic activity. Variations in field characteristics, fossil assemblages, and ichnofossil content highlight the lack of a direct hydrological connection between Aliabad and the main Qom sedimentary basin.

These differences are rooted in tectonic timing. The Aliabad sediments formed during the Eocene, under the influence of compressional and extensional phases of the Laramide Orogeny and associated magmatism, which created localized basins such as pull-apart structures along the Ravand Fault [40]. This predates the regional Pyrenean Orogeny and the subsequent Oligo-Miocene marine transgression responsible for deposition of the Qom Formation.

#### Broader implications and economic potential

The results establish the Aliabad succession as an Eocene composite volcaniclastic—carbonate system, distinct from the overlying Qom Formation. This recognition resolves long-standing stratigraphic uncertainties and underscores the tectonically active paleogeography of Central Iran during the late Eocene, when terrestrial, lacustrine, and short-lived marine environments coexisted in a dynamic volcanic setting.

In addition to its stratigraphic and paleoenvironmental significance, the succession holds economic implications. Lacustrine systems are known for hydrocarbon potential, and the presence of evaporites (halite, carnallite) and iron-rich phases (hematite) points to possible resource prospects that merit targeted exploration.

In summary, the Aliabad succession represents a tectonically driven, volcanically dominated lacustrine basin with episodic marine connections. Its late Eocene age and distinctive lithological and diagenetic characteristics unambiguously differentiate it from the Oligo-Miocene Qom Formation, reflecting divergent basin histories within Central Iran.

#### **European analogues and basin comparisons**

This section contrasts the Eocene lacustrine—volcaniclastic deposits of Aliabad with two European analogues: the Thrace Basin (European Turkey/NE Greece/Bulgaria) and the Messel Formation in Germany (Table S6). The Thrace Basin represents a forearc basin with extensive Eocene to Oligocene clastic sediments and volcaniclastic input, whereas the Aliabad deposits formed within the Urumieh—Dokhtar volcanic belt of central Iran, which formed along an active continental margin during the Eocene. The Messel Formation is a different endmember – a small maarlake deposit dominated by laminated oil shales and exceptional fossil preservation.

The Thrace Basin provides a suitable European analogue for the Aliabad deposits because it is of comparable age (late Middle Eocene–Oligocene), includes volcaniclastic tuffs, and shows a mix of marine and continental facies. Remote-sensing or GIS analysis could be used to compare the spatial distribution of depositional environments in the Thrace Basin with those inferred for Aliabad; for example, by mapping outcrops of tuffs and reefal carbonates using satellite imagery and correlating them to structural features (fault zones).

By contrast, the Messel Formation represents a different end-member: a small maar-lake deposit dominated by laminated oil shale. Its lake waters were permanently stratified and anoxic, leading to the exceptional preservation of fossils. Including this contrast in the manuscript highlights how lacustrine systems can vary from large fore-arc basins like Thrace or Aliabad to isolated volcanic lakes, and demonstrates the importance of volcanic setting, basin size, and hydrology in controlling sedimentary facies.

Acknowledgment: The authors would like to express their sincere gratitude to Dr. Benyamin Karimi, Mr. Saeed Haj-Amini, Ms. Zeynab Heydarifard, Mr. Mohammad-Ali Mim-Barqi, Dr. Fereshteh Sajjadi, Dr. Mohsen Eliassi, Dr. Jahanbakhsh Daneshian, Dr. Ebrahim Ghasemi Nejad and Dr. Faramarz Tooti for their valuable guidance, technical support, and insightful discussions throughout the course of this research. We are also deeply thankful to the administration and staff of the Department of Geology at the University of Tehran and Company Exploration Directorate for their continued cooperation, logistical assistance and providing several thin sections of the Qom Formation of the region, which greatly facilitated the completion of this study. The authors used Grammarly ® and generative Al assistant for minor language and style editing. All scientific content and interpretations were prepared and verified by the authors.

#### References

- 1. 372, I.O.D.P.I.E., *Methods: Sample preparation and analytical procedures*, in *Expedition Reports*. 2018, International Ocean Discovery Program.
- 2. Abbassi, N. and A. Amini, *Thalassinoides Ichnofabric from Oligocene Sediments in the Ali Abad Section, Qom Area, Central Iran.* Scientific Quarterly Journal of Geosciences, 2008. **18**(69): p. 86–101.
- 3. Afshar-Harb, A. and A. Houshmandzadeh, *Geology of Iran: Geology of Kopet Dagh*. Geology of Iran. Vol. 11. 1994, Tehran: Geological Survey of Iran.
- 4. Afshin, S., Sedimentary environment of sections E and F of the Qom Formation in Navab Anticline between Ghamsar and Kashan based on microfacies studies, trace elements, and X-ray, in Faculty of Science. 1995, University of Tehran.
- 5. Aghanabati, S.A., *Geology of Iran*. 2004, Tehran: Geological Survey of Iran. 707.
- 6. Allen, M., J. Jackson, and R. Walker, *Late Cenozoic reorganization of the Arabia-Eurasia collision and the comparison of short-term and long-term deformation rates*. Tectonics, 2004. **23**(2).
- 7. Allen, M.B., et al., *Right-lateral shear across Iran and kinematic change in the Arabia–Eurasia collision zone*. Geophysical Journal International, 2011. **184**(2): p. 555–574.
- 8. Armstrong-Altrin, J.S., Evaluation of two multi-elemental ratios as proxies for discriminating different tectonic settings of sandstones. Sedimentary Geology, 2015. **326**: p. 22–34.
- 9. Armstrong-Altrin, J.S. and S.P. Verma, *Critical evaluation of major- and trace-element geochemistry in distinguishing tectonic settings of sandstones.* Chemical Geology, 2005. **216**(3-4): p. 347–368.
- 10. Behjati, M., Petrographic, diagenetic, sedimentary environment, and paleoecology study of the limestone facies of sub-member c1 of the Qom Formation in Joodaj section (SW Kashan), in Faculty of Science. 2000, University of Tehran.
- 11. Berberian, F. and M. Berberian, *Tectono-plutonic episodes in Iran*, in *Zagros, Hindu Kush, Himalaya: Geodynamic Evolution*, H.K. Gupta and F.M. Delany, Editors. 1981, American Geophysical Union: Washington, DC. p. 323.

- 12. Bina, M.M., et al., *Palaeomagnetism, petrology and geochronology of Tertiary magmatic and sedimentary units from Iran*. Tectonophysics, 1986. **121**: p. 303–329.
- 13. Bozorgnia, F., *Qom Formation stratigraphy of the Central Basin of Iran and its intercontinental position*. Bulletin of the Iranian Petroleum Institute, 1966. **24**: p. 69–75.
- 14. Daneshian, J. and L.R. Dana, *Early Miocene benthic foraminifera and biostratigraphy of the Qom Formation, Deh Namak, Central Iran*. Journal of Asian Earth Sciences, 2007. **29**(5): p. 844–858.
- 15. Darvishzadeh, A., Geology of Iran. 1991, Tehran: Amirkabir University.
- 16. Dickson, J.A.D., *A Modified Staining Technique for Carbonate in the Thin Section*. Nature, 1965. **205**(4971): p. 587.
- 17. Dozy, J.J., Comments on geological report No. 1, by Thiebaud (on Qum-Saveh area. 1944, Geological Survey. p. 308.
- 18. Dozy, J.J., *A sketch of post-Cretaceous volcanism in central Iran*. Leidse Geologische Mededelingen, 1955. **20**(1): p. 48–57.
- 19. Emami, M.H., Géologie de la région de Quom-Aran (Iran). Contribution à l'étude dynamique et géochimique du volcanisme tertiaire de l'Iran central. 1981, Université Joseph-Fourier Grenoble I.
- 20. Farzaneh, R., Sedimentary environment study of the volcaniclastic sediments of Aliabad area (Qom highway)., in Faculty of Science. 1998, University of Tehran.
- 21. Farzaneh, R. and O. Rasool, *Petrology of Pyroclastic Volcaniclastic Deposits in the Aliabad Region*, in *The 2nd Conference of the Geological Society of Iran*. 1998.
- 22. Fisher, R.V. and H.-U. Schmincke, *Pyroclastic Rocks*. 1 ed. 1984: Springer-Verlag Berlin Heidelberg. 472.
- 23. Flügel, E., *Microfacies of Carbonate Rocks. Analysis, Interpretation and Application*. 2010: Springer Berlin, Heidelberg. 984.
- 24. Furrer, M. and P. Soder. The oligo-Miocene marine formation in the Qom region (central Iran). in Proceedings of the 4th world petroleum congress, Rome, Section I/A/5. 1955.

- 25. Gansser, A. New Aspects of the Geology in Central Iran (Iran). in 4th World Petroleum Congress. 1955.
- 26. Guest, B., et al., Late Cenozoic shortening in the west-central Alborz Mountains, northern Iran, by combined conjugate strike-slip and thin-skinned deformation. Geosphere, 2006. **2**(1): p. 35–52.
- 27. Haddadan, M., *Geological map of Zaviyeh quadrangle*. 2005, Geological Survey of Iran: Tehran.
- 28. Haj Amini, S., Internal report of Peynegar Gomaneh Company on earthquake hazard analysis of Qom road tunnel in the inflection zone. 2011: Tehran/Qom.
- 29. Hajian, J., Geology of Iran (Paleocene–Eocene in Iran). 1996, Tehran: Geological Survey of Iran.
- 30. Hong, C., et al., Weathering and alteration of volcanic ashes in sedimentary environments: Mineralogical and geochemical constraints. Chemical Geology, 2017. **466**.
- 31. Huber, H., Geological report on the Upper Qara-Chai area between Saveh and Hamadan. Tehran, Iran: Iranian Oil Company Geological Report, 1952.
- 32. Jaafari, A. History and development of the Alborz and Sarajeh fields of Central Iran. in World Petroleum Congress. 1963. WPC.
- 33. Karimi, A. and E. Rastad, Sedimentary facies, diagenetic evolution and mineralizing environments of the Nakhirkooh celestite deposit, Varamin. Scientific Quarterly Journal of Geosciences, 1999. **33**: p. 20–33.
- 34. Karimi, M., Petrological characteristics and environmental conditions of the volcaniclastic–carbonate mixed rocks of Aliabad region and investigation of their relationship with the Qom sedimentary basin., in Faculty of Geology. 2016, University of Tehran.
- 35. Karunarathne, P.W.G.L., D.E.C. Jayawardena, and H.M.T.G.A. Pitawala, *Clay mineralogy and petrogenesis of tuffaceous sedimentary rocks using powder X-ray diffraction analyses*. Journal of Asian Earth Sciences, 2024. **263**.
- 36. Khodaparast, S., Structural analysis of the Dokhan area (west of Saveh) with an emphasis on the thickness variations of the Qom Formation., in Faculty of Basic Sciences. 2009, Tarbiat Modares University: Tehran.

- 37. Khodaparast, S., M. Mohajjel, and S.H. Amini, *Structural analysis of the Dokhan area* (west of Saveh) with an emphasis on the thickness variations of the Qom Formation. . Scientific Quarterly Journal of Geosciences, 2012. **24**(93): p. 235–0.
- 38. Letouzey, J. and J. Rudkiewicz, *Structural geology in the Central Iranian Basin*. Institut Français du Petrole report F, 2005. **214001**: p. 79.
- 39. McHenry, L.J., A.D. Pollington, and M.D. Smith, *Mineralogical and geochemical fingerprinting of tuff and tuffite units in sedimentary successions*. Sedimentary Geology, 2021. **420**.
- 40. Mohajjel, M., & Rahami, Z., Structure of ravand fault and its role on extensional pull-apart basin in oromieh-dokhtar volcanic belt. Iranian Journal Of Geology, 2009. **3**(11): p. 39–45.
- 41. Morley, C.K., et al., Structural development of a major late Cenozoic basin and transpressional belt in central Iran: The Central Basin in the Qom-Saveh area. Geosphere, 2009. **5**(4): p. 325–362.
- 42. Mormone, A., R. De Gennaro, and M. Piochi, *Mineralogical, geochemical and isotopic features of Neapolitan Yellow Tuff and related tuffs: Implications for alteration processes*. Journal of Volcanology and Geothermal Research, 2015. **301**: p. 150–163.
- 43. Nogol-e-Sadat, M., *Tectonics and geology of the Qom area*, in *Faculty of Science*. 1973, University of Tehran: Tehran.
- 44. Nogol-e-Sadat, M., Structural shear and bending regions in Iran: Structural analysis results of the Qom area. 1985, Geological Survey of Iran: Tehran.
- 45. Nogol-e-Sadat, M.A.A. and M. Almasian, *Tectonic Map of Iran*. 1993, Geological Survey of Iran: Tehran.
- 46. Okhravi, R. and A. Amini, *An example of mixed carbonate–pyroclastic sedimentation* (*Miocene, Central Basin, Iran*). Sedimentary Geology, 1998. **118**(1): p. 37–54.
- 47. Qurbānī, M.o., *The economic geology of Iran : mineral deposits and natural resources*. 2013, Netherlands: Dordrecht : Springer.
- 48. Rahimzadeh, F., *Geology of Iran, Oligocene, Miocene, Pliocene.* 1994: Geological Survey and Mineral Exploration Organization.

- 49. Reuter, M., et al., The Oligo-/Miocene Qom Formation (Iran): evidence for an early Burdigalian restriction of the Tethyan Seaway and closure of its Iranian gateways. International Journal of Earth Sciences, 2009. **98**(3): p. 627–650.
- 50. Rollinson, H.R. and E. 2nd, *Using geochemical data: Evaluation, presentation, interpretation.* 2nd ed. 2020: Elsevier.
- 51. Salarifar, M., Petrography, sedimentary environment, and diagenesis of the Doboradar reef in Qom., in Department of Geology. 1991, University of Tehran.
- 52. Schuster, F. and U. Wielandt, *Oligocene and Early Miocene coral faunas from Iran:* palaeoecology and palaeobiogeography. International Journal of Earth Sciences, 1999. **88**(3): p. 571–581.
- 53. Stöcklin, J., Structural History and Tectonics of Iran1: A Review. AAPG Bulletin, 1968. **52**(7): p. 1229–1258.
- 54. Survey, U.S.G. *EarthExplorer*. 2025 [cited 2025 18 September]; Available from: https://earthexplorer.usgs.gov/.
- 55. Tucker, M.E., Sedimentary petrology: an introduction. Second ed. 1994: John Wiley & Sons.
- 56. Vagenas, N.V., et al., *Quantitative analysis of synthetic calcium carbonate polymorphs using FT-Raman spectroscopy.* Talanta, 2003. **59**(4): p. 831–836.
- 57. Verma, S.P. and J.S. Armstrong-Altrin, *Geochemical discrimination of siliciclastic sediments from active and passive margin settings*. Sedimentary Geology, 2016. **333**: p. 67–75.
- 58. Vincent, S.J., et al., Oligocene uplift of the Western Greater Caucasus: an effect of initial Arabia–Eurasia collision. Terra Nova, 2007. **19**(2): p. 160–166.
- 59. Zahedi, M., Étude géologique de la région de Soh (W. de l'Iran central). 1971, Université Claude Bernard-Lyon I. p. 278.
- 60. Zimmerle, W., Petroleum Sedimentology. 1995: Springer Netherlands.
- 61. Zuffa, G.G., *Hybrid arenites; their composition and classification*. Journal of Sedimentary Research, 1980. **50**(1): p. 21–29.

62. Zuffa, G.G., Optical Analyses of Arenites: Influence of Methodology on Compositional Results, in Provenance of Arenites, G.G. Zuffa, Editor. 1985, Springer Netherlands: Dordrecht. p. 165–189.

# **Appendix A: Supplementary Figures and Tables**

# Eocene lacustrine-volcaniclastic deposits at Aliabad (Central Iran): A possible Proto-basin of the Oligo-Miocene Qom Formation

Λ		1	L	_		
А	u	ι	n	О	rs	0

Mahdokht Karimi<sup>1\*</sup>, Abdolhossein Amini<sup>1</sup>, Nasrollah Abbassi<sup>2</sup>, Mohsen Ranjbaran<sup>1</sup>

#### Affiliations:

- 1. School of Geology, College of Science, University of Tehran, Iran
- 2. Department of Geology, Faculty of Science, University of Zanjan, Zanjan, Iran

This document contains 1 Figure (S1) and 6 tables (S1-S6).

<sup>\*</sup> Corresponding author: Mahdokht Karimi, Department of Geology, School of Science, University of Tehran, Iran. E-mail: m19 karimi@ut.ac.ir

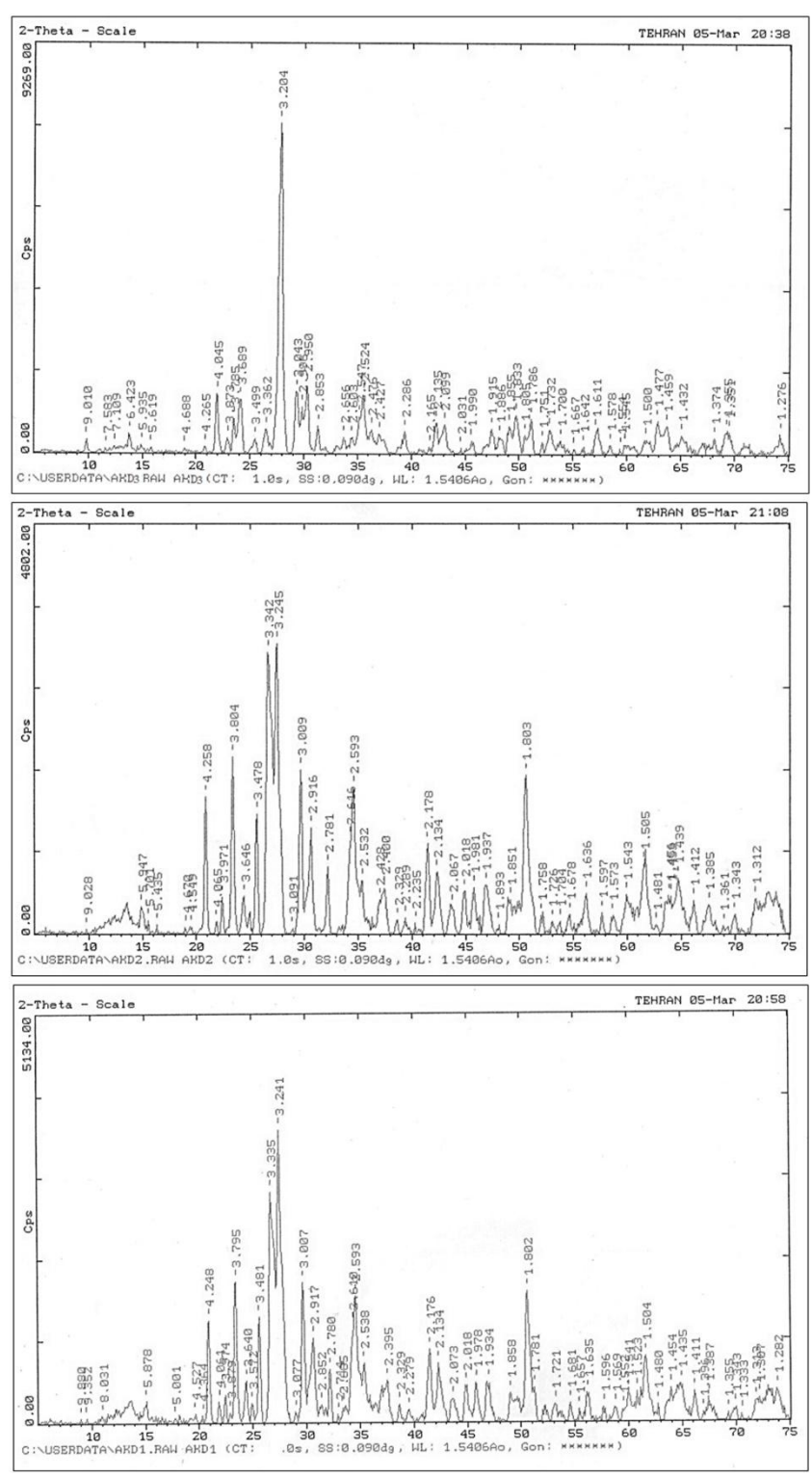


**Figure S1:** Diagram resulting from X-ray diffraction (XRD) analysis conducted on fine-grained sedimentary facies.

Table S1. Three Samples' Minerals Identified by XRD Analysis Results.

Sample 2

Microcline: KAlSi<sub>3</sub>O<sub>8</sub>
Orthoclase: (K,Ba)(Al,Si)<sub>4</sub>O<sub>8</sub>
Sericite: KAl<sub>2</sub>(AlSi<sub>3</sub>)O<sub>10</sub>(OH)<sub>2</sub>
Albite: NaAlSi<sub>3</sub>O<sub>8</sub>
Analcim: NaAl(Si<sub>2</sub>O<sub>6</sub>)·H<sub>2</sub>O
Kaolinite: Al<sub>2</sub>Si<sub>2</sub>O<sub>5</sub>(OH)<sub>4</sub>
Quartz: SiO<sub>2</sub>
Halite: NaCl
Hematite: Fe<sub>2</sub>O<sub>3</sub>
Carnallite: KMgCl<sub>3</sub>·6H<sub>2</sub>O

Albite: NaAlSi<sub>3</sub>O<sub>8</sub>
Analcime: NaAl(Si<sub>2</sub>O<sub>6</sub>)·H<sub>2</sub>O
Sericite: KAl<sub>2</sub>Si<sub>3</sub>AlO<sub>10</sub>(OH)<sub>2</sub>
Kaolinite: Al<sub>2</sub>Si<sub>2</sub>O<sub>5</sub>(OH)<sub>4</sub>
Hematite: Fe<sub>2</sub>O<sub>3</sub>
Carnallite: KMgCl<sub>3</sub>·6H<sub>2</sub>O
Halite: NaCl
Magnetite:
(Fe,Mg)(Al,Cr,Fe,Ti)<sub>2</sub>O<sub>4</sub>

Albite: NaAlSi<sub>3</sub>O<sub>8</sub>
(Na,Ca)(Si,Al)<sub>4</sub>O<sub>8</sub>
Calcite: CaCO<sub>3</sub>
Hematite: Fe<sub>2</sub>O<sub>3</sub>
Illite:
K<sub>0·5</sub>(Al,Fe,Mg)<sub>3</sub>(Si,Al)<sub>4</sub>O<sub>10</sub>(OH)<sub>2</sub>
Quartz: SiO<sub>2</sub>
Clinoptilolite:
KNa<sub>2</sub>Ca<sub>2</sub>(Si<sub>29</sub>Al<sub>7</sub>)O<sub>72</sub>·32H<sub>2</sub>O

Sample 3

**Table S2.** The examination and frequency analysis of different types of tuff rocks in 46 studied sections from this area have led to the following results. (C = Crystal, L = Lithic, V = Vitric, T = Tuff).

		Abundance (%)						
Sections	LCT	CLT	LVT	VCT	CVT	СТ	Total Volcaniclastic component	
Section A	40	10	-	-	50	-	58.5	
Section B	12.50	6.25	6.25	12.5	43.75	18.75	68.125	
Section C	35.29	64.70	-	-	-	-	73.82	
Section D	66.67	-	-	-	33.33	-	81.66	
Average/section	30.43	28.26	2.17	4.35	28.26	6.52		
Rank of Abundance	1	2	5	4	2	3		
Average Percentage of Volcaniclastic Component Across the Entire Area			69.0	2 %				

Table S3. XRF Chemical Analysis Results (Oxides)

Order		Abundance (%)	
Oxides	Sample 1	Sample 2	Sample 3
SiO2	58.21	58.63	48.01
Al2O3	16.56	16.41	10.52
Fe2O3	3.93	5.99	5.28
CaO	1.51	1.87	14.96
Na2O	1.63	0.59	3.89
K2O	7.81	7.83	0.52
MgO	1.26	1.69	0.27
TiO2	0.604	0.615	0.632
MnO	0.073	0.151	0.185
P2O5	1.169	0.178	0.124
S	0.019	0.052	0.052
L.O.I	8.05	15.28	15.28

Table S4. XRF Chemical Analysis Results (Trace Elements in ppm)

Trace	А	bundance p	om	Trace	,	Abundance p	pm
element	Sample 1	Sample 2	Sample 3	element	Sample 1	Sample 2	Sample 3
CI	74	62	101	W	7	2	6
Ва	1363	1413	194	Zr	96	232	211
Sr	826	475	492	Y	107	100	21
Cu	147	170	138	Rb	376	351	24
Zn	99	107	126	Со	6	9	8
Pb	7	12	26	As	8	24	42
Ni	32	34	32	U	7	9	2
Cr	8	9	8	Th	9	12	3
V	87	87	147	Мо	4	2	3
Ce	35	71	19	Ga	14	15	9
La	16	32	11	Nb	1	1	2

**Table S5.** Brief Description of Qom Formation Stratigraphic Units in South Koushk-e Nosra, Including Correlative Equivalents and Thickness Estimates (19).

Probable Equivalent	Layer Description			
Upper Red Formation	Abrupt appearance	1		
Sub-member c1	Sandy Limestone (RMF15) – Light – Contains clastic fragments of porphyritic andesite in sand size – Initially coarsening upward then fine to gravel – Fragments – First few centimeters contain mud clasts – Very abundant fossils – Contains stylolites and calcite-filled fractures.	~700 cm		
	Limestone – Lacking distinct structure – Fine-grained – Light.	~15 cm		
	Sandy Limestone – Light brown – Lacking fossils in hand sample – Contains bioturbation – Rough to touch – Onion-skin weathering.	~60 cm		
Member b	Limestone – Light – Contains sandy interlayers, with a brown structure – In the range of 20 to 45 cm, with cross-bedding – Shape and siliceous cement as quartz crystals in some lenses – Surfaces – Fine-grained – With a weathered appearance – As depressions.	~2000 cm		
Member a	Limestone (RMF14) – Light – Contains fossil fragments – Vertical worm tubes on the layer surface – Stylolites – Fine debris and fossil fragments filled with granular limestone – Perpendicular fractures – Which have created weathered planes of weakness and thus an irregular layered appearance.	~80 cm		
Eocene Volcanics	Without LRF presence – Has a gradual boundary with Qom Formation sediments.	-		

Table S6. Key attributes of the Aliabad deposits and European analogues

Attribute	Aliabad (Central Iran)	Thrace Basin (European Turkey/NE Greece/Bulgaria)	Messel Formation (Germany)
Age and geological setting	Eocene; interpreted as a lacustrine—volcaniclastic basin adjacent to the younger Oligo–Miocene Qom Formation deposits in the Aliabad region.	Formed in the late Middle Eocene to latest Oligocene; a fore-arc basin developed above the Intra-Pontide subduction zone. It contains about 9 km of Eocene–Miocene marine and continental clastics overlying Paleozoic– Mesozoic basement [2, 3].	Middle Eocene (~47 Ma); a maar-lake deposit restricted to the Messel pit in Hesse, Germany. The formation unconformably overlies Permian basement and Eocene volcanic breccias [1].
Sedimentary succession and thickness	In total ~280 m of volcaniclastic-carbonate hybrid arenites, mudstones and marls with abundant volcaniclastics (~69 %) and lacustrine to marginal-marine facies (summarized from the Aliabad study).	Up to 9 km of interbedded fine- to coarse-grained clastics deposited in a variety of environments including turbidites, muddy carbonates with local reef development, river channels and tuffs [3, 4].	~200 m of laminated bituminous shale ("oil shale") deposited in an anoxic lake; overlain by minor volcanic breccias. The oil shale succession extends ~13 m downward and lies above basaltic sandstone [1].
Volcanic influence	Volcaniclastic grains dominate the sand–silt fraction; zeolite minerals (analcime, clinoptilolite) record interaction with volcanic ash; pyroclastic input sourced from nearby volcanic centres.	Eocene magmatism produced andesitic and dacitic tuffs within the basin; the sedimentary fill includes tuffs and volcaniclastics interbedded with marine and continental clastics [3].	Deposition occurred in a maar-lake created by phreatomagmatic explosions. The formation overlies volcanic breccias and contains basaltic fragments; however, the lacustrine shale itself records little clastic influx and is dominated by autochthonous organic sediment [1].
Depositional environment	Lacustrine with episodic marine incursions; hybrid arenites reflect mixing of shallow-marine carbonates and volcaniclastic detritus; ichnofossils (e.g., Thalassinoides) and evaporitic minerals suggest brackish to saline conditions.	Mixed marine and continental; includes turbidites, reefal carbonates, deltaic sandstones and fluvio-lacustrine deposits. The basin evolved from deep-marine to marginal-marine and continental settings during the Eocene–Oligocene [4].	A permanently stratified maar-lake with anoxic bottom waters. Oil shale formed from slow deposition of organic-rich mud and dead vegetation; periodic overturning of lake waters caused die-offs of aquatic species and exceptional fossil preservation [1].
Key minerals and fossils	Zeolites (analcime, clinoptilolite), evaporites (halite, carnallite), hematite; ichnofossils indicative of	Reefal limestones, turbiditic sandstones and tuffs; economic hydrocarbon source rocks (Hamitabat and Mezardere shales). Fossils	Laminated oil shale with exquisitely preserved fossils of mammals, birds, reptiles, insects and

	shallow-marine incursions.	include plant remains and ostracods in fluvio-lacustrine units [4].	plants; indicates anoxic, low-energy conditions [1].
Implications for Aliabad comparison	Provides the baseline for a lacustrine—volcaniclastic basin with significant volcanic input and mixed facies.	Similarities: Both basins formed in the Eocene and contain interbedded volcaniclastics and marine/continental sediments. The Thrace Basin's thick succession and tuffs demonstrate that volcanic eruptions influenced sedimentation. Differences: The Thrace Basin is much thicker (kilometre-scale), has a fore-arc tectonic setting and transitions from marine to fluvio-lacustrine environments.	Different end-member: The Messel Formation is a small maar-lake deposit dominated by laminated oil shale with minimal clastic input. It lacks the mixed carbonate—volcaniclastic facies of Aliabad and Thrace, and instead highlights an anoxic, stratified lacustrine system with spectacular fossil preservation

#### References

- 1. Franzen, J.L. and M. Röper, *The Messel oil shale deposit: Geology and paleontology of a Middle Eocene maar lake deposit in Hesse, Germany.* International Journal of Earth Sciences, 1997. **86**(3): p. 361–375.
- 2. Görür, N. and A.I. Okay, *A fore-arc origin for the Thrace Basin, NW Turkey.* Geologische Rundschau, 1996. **85**: p. 662–668.
- 3. Okay, A.I. and N. Görür, *Tectonic evolution and sedimentary record of the Thrace Basin, northwestern Turkey: A forearc basin example.* Tectonophysics, 1997. **270**(1–3): p. 211–232.
- 4. Tüysüz, O., K. Şentürk, and Y. Yilmaz, *Tectonic evolution of the Thrace Basin and its hydrocarbon potential*. Turkish Journal of Earth Sciences, 1998. **7**: p. 1–25.